

研究成果の刊行物・別刷

Neocortical Layer Formation of Human Developing Brains and Lissencephalies: Consideration of Layer-Specific Marker Expression

Takashi Saito^{1,2}, Sae Hanai^{1,2}, Sachio Takashima³, Eiji Nakagawa², Shin Okazaki⁴, Takeshi Inoue⁵, Rie Miyata⁶, Kyoko Hoshino⁷, Takumi Akashi⁸, Masayuki Sasaki², Yu-ichi Goto¹, Masaharu Hayashi⁶ and Masayuki Itoh¹

¹Department of Mental Retardation and Birth Defect Research, National Center of Neurology and Psychiatry, Kodaira, 187-8502, Japan, ²Department of Child Neurology, The Hospital of National Center of Neurology and Psychiatry, Kodaira, 187-8551, Japan, ³Yanagawa Institute of Handicapped Children, International University of Health and Welfare, Fukuoka, 832-0058, Japan, ⁴Department of Pediatrics, Osaka City General Hospital, Osaka, 534-0021, Japan, ⁵Department of Pathology and Laboratory Medicine, Osaka City General Hospital, Osaka, 534-0021, Japan, ⁶Department of Clinical Neuropathology, Tokyo Metropolitan Institute of Neuroscience, Fuchu, 183-8526, Japan, ⁷Department of Pediatrics, Saitama Medical Center, Kawagoe, 350-8550, Japan and ⁸Department of Pathology and Laboratory Medicine, Tokyo Medical and Dental University, Tokyo, 113-8510, Japan

Takashi Saito and Masayuki Itoh have contributed equally to this work.

Address correspondence to M Itoh, Department of Mental Retardation and Birth Defect Research, National Center of Neurology and Psychiatry, 4-1-1 Ogawahigashi, Kodaira, Tokyo 187-8502, Japan. Email: itoh@ncnp.go.jp.

To investigate layer-specific molecule expression in human developing neocortices, we performed immunohistochemistry of the layer-specific markers (TBR1, FOXP1, SATB2, OTX1, CUTL1, and CTIP2), using frontal neocortices of the dorsolateral precentral gyri of 16 normal controls, aged 19 gestational weeks to 1 year old, lissencephalies of 3 Miller-Dieker syndrome (MDS) cases, 2 X-linked lissencephaly with abnormal genitalia (XLAG) cases, and 4 Fukuyama-type congenital muscular dystrophy (FCMD) cases. In the fetal period, we observed SATB2+ cells in layers II-IV, CUTL1+ cells in layers II-V, FOXP1+ cells in layer V, OTX1+ cells in layers II or V, and CTIP2+ and TBR1+ cells in layers V and VI. SATB2+ and CUTL1+ cells appeared until 3 months of age, but the other markers disappeared after birth. Neocortices of MDS and XLAG infants revealed SATB2+, CUTL1+, FOXP1+, and TBR1+ cells diffusely located in the upper layers. In fetal FCMD neocortex, neurons labeled with the layer-specific markers located over the glia limitans. The present study provided new knowledge indicating that the expression pattern of these markers in the developing human neocortex was similar to those in mice. Various lissencephalies revealed abnormal layer formation by random migration.

Keywords: developing human neocortex, layer-specific marker, lissencephaly

Introduction

The experimental neurosciences have recently provided many new insights into the molecular mechanisms of mammalian cerebral formation. Past knowledge revealed that some molecules are regulated with a well-designed genetic algorithm during the developmental stages, with interrelated phenomena that include cell proliferation, fate determination and migration to the proper laminar, and final position in the cerebral cortex. Neocortical laminar formation is highly programmed by genetic control in the early embryonic period. At the decided time, projection neurons migrate into the cortical plate (CP) along the radial glial process from the subventricular germinal zone with an inside out pattern. At this neural migration stage, integration of reelin (RELN), Lis-1, doublecortin (DCX), and other molecules is required to form a complete neocortex (Guillemot et al. 2006; Mochida and Walsh 2004). Finally, mammalian brains commonly show a 6-layer neocortex, and

each layer has a specific function with a synaptic connection. In each step, specific genes have important roles, and the molecular mechanism is well known in rodent brains (Arlotta et al. 2005; Alcamo et al. 2008). *Satb2*, a special AT-rich binding protein 2, generates callosal projection neurons in layers II-IV (Alcamo et al. 2008; Britanova et al. 2008). *Ctip2*, encoding a C2H2-type zinc finger protein, locates in layers V and VI and promotes corticospinal motor neuron projection (Arlotta et al. 2005; Britanova et al. 2008). *Satb2* is a repressor of *Ctip2* and makes not only the callosal projection but also the subcortical connections (Alcamo et al. 2008). Mouse *Otx1*, orthodenticle homeobox 1, is expressed in a number of cells in layers V and VI (Weimann et al. 1999). *Tbr1*, a member of the T-box homeobox gene family, expresses in preplate and layer VI in mouse fetal brain (Hevner et al. 2001) and layers I-III and layer VI in mouse adult brain (Bulfone et al. 1995). *Tbr1* contributes to make corticocortical projection neurons (Hevner et al. 2001). *Tbr1* expresses in the deep layer of the human fetus cortex (Sheen et al. 2006). A transcription factor *Cutl1*, drosophila homeobox CUT like 1, is expressed in pyramidal neurons of the upper layer (Nieto et al. 2004). *Foxp1*, a transcription factor of the winged-helix/forkhead family, expresses in layers III-V of mouse neocortex (Ferland et al. 2003) and layer V in human neocortex (Sheen et al. 2006). *Foxp1* expresses in the deep layer of Miller-Dieker syndrome (MDS) neocortex (Sheen et al. 2006). However, many rodent studies show that the other layer-specific molecules also play very important roles in forming cortical lamination (Molyneaux et al. 2007) and that such gene disruption leads to profound cortical malformation (Mochida and Walsh 2004).

Lissencephaly, formed at the neuronal migration period, is classically recognized to be mainly of 2 types; smooth pachygyria-agyria as type I lissencephaly and cobblestone lissencephaly as type II lissencephaly (Olson and Walsh 2002). Type I (classical) lissencephaly shows a thick 4-layer cortex and is typically known as MDS and double cortex syndrome. The causative genes of type I lissencephaly are known as RELN, Lis-1, DCX, and filamine. Interestingly, the gene products are associated with the microtubules and can alter the cytoskeleton size for cell movement (de Rouvroit and Goffinet 2001; Reiner and Sapir 2009) or its related molecules (Olson and Walsh 2002; Assadi et al. 2003). Typical type II (cobblestone) lissencephalies

of Muscle-eye-brain disease, Walker-Warburg syndrome (WWS), and Fukuyama-type congenital muscular dystrophy (FCMD), are caused by mutated genes encoding enzymes of alpha-dystroglycan glycosylation, such as POMGnT1, protein-O-mannosyltransferase (POMT) 1 and 2, and Fukutin, respectively (Mochida and Walsh 2004). The posttranslational glycosylated alpha-dystroglycan binds to extracellular matrix (Michele et al. 2002). Reduction of glycosylation leads to disruption of the glia limitans over which neurons migrate (Yamamoto et al. 2004).

Recently, it has been reported that X-linked lissencephaly with abnormal genitalia (XLAG), whose causative gene is *Aristaless*-related homeobox gene (*ARX*), is a new type of lissencephaly that shows a 3-layer neocortex (Dobyns et al. 1999; Kitamura et al. 2002; Bonneau et al. 2002; Okazaki et al. 2008). *ARX* has a homeodomain and decides the migration of interneurons in the ganglionic eminence. However, it is unknown why *ARX* dysfunction leads to abnormal radial neuronal migration in human XLAG, whereas *ARX*-null mice show reduced cortical proliferation but normal migration (Kitamura et al. 2002; Okazaki et al. 2008).

It is very important to reveal the molecular and morphological relationship between these malformed brains to understand human neocortical formation and pathophysiology, although little is known about the expression pattern of layer-specific markers in human developing brain (Hevner 2007). In the present study, we focus on layer formation and investigate the expression of layer-specific molecules in neocortices of human developing brains and lissencephalies.

Materials and Methods

Human Brain Tissues

All cerebral tissues used in the present study were approved for research usage by parents and Ethical Committees of the involved hospitals and institutes. For the developmental study, we used frontal cortices of the dorsolateral precentral gyri of 16 controls, showing no neuropathological findings (age 19 gestational weeks [GWs] to 1 year after birth) (Supplementary Material). In addition, we examined the same frontal cerebral hemispheres of lissencephaly, which were clinicopathologically diagnosed as MDS, XLAG, and FCMD (Supplementary Material). The postmortem interval (time from death to fixation) of all subjects was within 12 h (Supplementary Material). After removal, all brains were fixed in 10% buffered formalin or 4% paraformaldehyde for 2 weeks. Then, brains were dehydrated with 70–100% alcohol and embedded in paraffin. The serial sections were cut 6 μ m thick for histological and immunohistological examination.

Histology and Immunohistochemistry

For investigation of brain architecture, the sections were stained with hematoxylin and eosin (HE) and Klüber-Barrera (KB) method. To investigate cortical layer formation, we performed immunohistochemistry using cortical layer-specific markers; polyclonal antibodies against TBR1 (dilution of 1:100; Abcam), FOXP1 (1:100; Abcam), and OTX1 (1:100; Abcam), as well as monoclonal antibodies against SATB2 (1:100; Bio Matrix Research Inc.), CUTL1 (1:100; Abnova), and CTIP2 (1:20; Abcam).

Our immunohistochemistry technique was previously described (Okazaki et al. 2008). Briefly, the serial sections were deparaffinized and rehydrated. For antigen retrieval, we performed an autoclave treatment (120 °C for 10 min in 10 mM citrate buffer, pH 6.0). Sections were incubated in primary antibodies at 4 °C for overnight, and then reacted with the secondary antibodies (Nichirei). We used amino ethyl carbazole (Nichirei) as a chromogen. For counterstaining, 0.2% methyl green was used. For double labeling, we used Alexafluor-488- and 568-conjugated secondary antibodies (Invitrogen Corporation) with

4',6'-diamidino-2-phenylindole (DAPI). We observed the stained tissues with FLUOVIEW 500 fluorescent microscope (Olympus).

Results

Cortical Lamination of Normal Developing Brains

Generally, we confirmed cortical formation of all subjects with HE- and KB-staining. We observed the CP and intermediate zone around 20 GW (Fig. 1A). At this embryonic period, SATB2+ cells located in the upper region of CP (Fig. 1B). CUTL1+ cells were diffusely distributed in CP (Fig. 1C). FOXP1+ cells were restricted to the middle region of CP (Fig. 1D). OTX1+ cells and CTIP2+ cells are seen in the lower region of CP (Fig. 1E,F). The distribution of TBR1+ cells exhibited a 2-layer pattern of CP and SP (Fig. 1G).

At approximately 30 GW, the neocortex was divided into 6 layers (Fig. 2A). The distribution of SATB2+ cells was observed in layers II–V, predominantly in layers II and IV (Fig. 2B). CUTL1+ cells were diffusely seen in layers II–VI (Fig. 2C). FOXP1+ cells were in layer IV and the upper region of layer V (Fig. 2D). OTX1+ cells were concentrated in layers IV and V (Fig. 2E). CTIP2+ and TBR1+ cells were located in layers V and VI (Fig. 2F,G). The developmental expression pattern is shown in Supplementary Figure 1.

In the perinatal period, the expression pattern of the cortical layer-specific markers is very similar to that of around 30 GW (Fig. 3). In the late gestational period, SATB2 expressed in the superficial region of the neocortex and CUTL1, FOXP1, and CTIP2 gradually demonstrated in the deep region, while TBR1 was in the bottom. Interestingly, OTX1+ cells were only in layer V (Fig. 3E). After birth, SATB2+ and CUTL1+ cells appeared until 3 months of age, although the other markers had already disappeared (data not shown).

In order to investigate the relationships among these layer-specific markers, we performed double fluorescent staining of SATB2 and FOXP1, SATB2 and TBR1, CTIP2 and SATB2, SATB2 and OTX1, CTIP2 and FOXP1, and CTIP2 and TBR1 (Fig. 4, Supplementary Figure 1). FOXP1+ and SATB2+ merged (FOXP1+/SATB2+) cells were observed in the superficial CP of 23 GW but in the deep layer after 29 GW (Fig. 4A). Throughout the fetal period, FOXP1+/CTIP2+ cells might be in the deep layer (Fig. 4E), and many SATB2+/OTX1+ cells were in layers II and IV or V (Fig. 4D). However, SATB2+ cells did not express CTIP2+ (Fig. 4C). TBR1+ cells had no SATB2, but there were a few CTIP2 signals in layer VI (Fig. 4B,F). The double staining of layer-specific marker expression was shown in Supplementary Figure 1.

Layer-Specific Marker Expression of Various Lissencephalies

MDS brains were typical agyria and pachygyria with thick cortex and thin white matter. MDS showed a 4-layer neocortex as previously reported (Crome 1956): a molecular layer, an external cellular layer (layer I), a sparsely cellular layer (layer II), and an internal cellular layer (layer III) (Fig. 5A). In layers II, III, and IV, small neurons, which had immunoreactivities of SATB2, CUTL1, FOXP1, and TBR1, were observed diffusely but were few in number (Fig. 5B–E). Large pyramidal neurons in the upper layer II had TBR1 (Fig. 5E). The neocortex in XLAG exhibited a 3-layer pattern (Bonneau et al. 2002): a molecular layer (layer I), an intermediate layer with densely packed

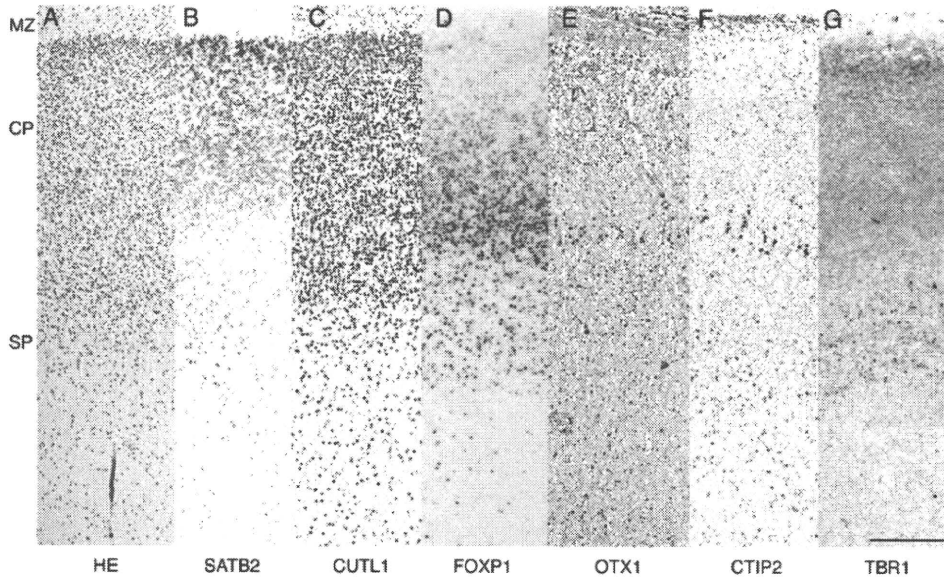


Figure 1. Layer-specific marker expression of the neocortex at 23 GWs. Around 20 GWs, the 3-layer pattern, that is, the marginal zone (MZ), CP, and subplate (SP), are seen (A). SATB2 expresses in the upper region of CP (B). CUTL1 diffusely expresses in the whole cortex and intermediate zone (C). FOXP1-positive cells locate in the middle region (D) and CTIP2-immunopositive cells (F) locate in the lower region of CP. OTX1 exhibits in CP and SP, predominantly lower region of CP (E). TBR1-immunopositive cells are in the lower region of CP and SP, as well as those fibers in CP (G). A, HE; B-G, SATB2, CUTL1, FOXP1, OTX1, CTIP2, and TBR1 immunohistochemistry, respectively. Scale bar: 100 μ m.

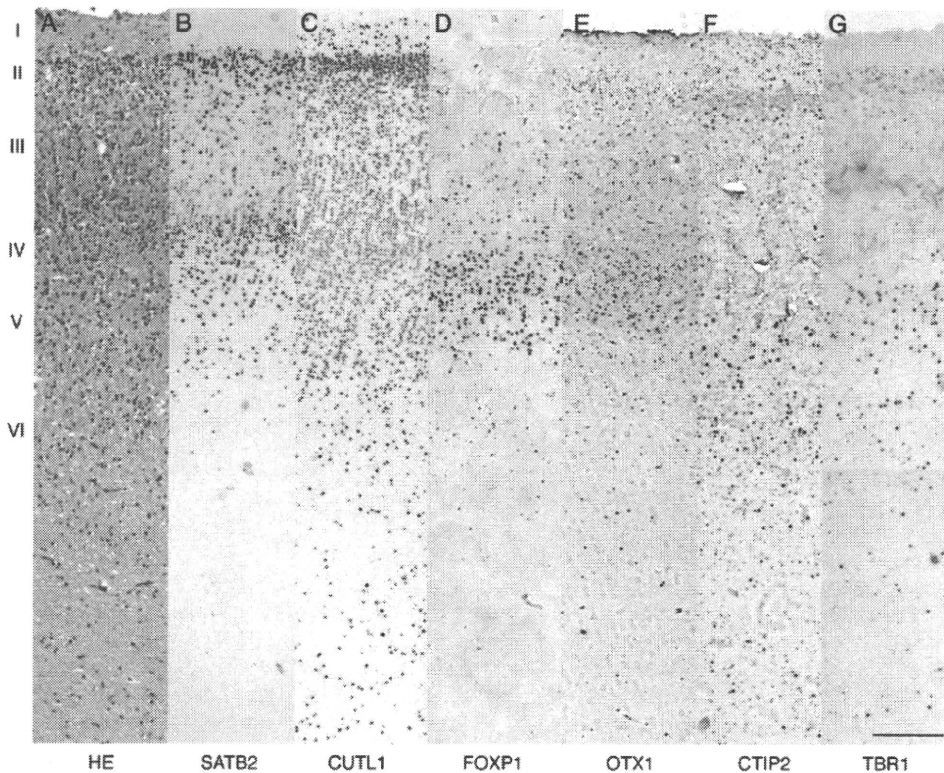


Figure 2. Layer-specific marker expression of the neocortex at 29 GWs. The 6-layer neocortex is shown (A). SATB2 expresses in layers II-V, especially layer II and upper region of layer IV (B). CUTL1 diffusely expresses in layers II-V and predominates in layer II (C). FOXP1 converges to layers VI and V (D). OTX expresses in upper layer and layers VI and V (E). CTIP2- and TBR1-immunopositive cells locate in layer V and layers V and VI (F and G). A, HE; B-G, SATB2, CUTL1, FOXP1, OTX1, CTIP2, and TBR1 immunohistochemistry, respectively. Scale bar: 100 μ m.

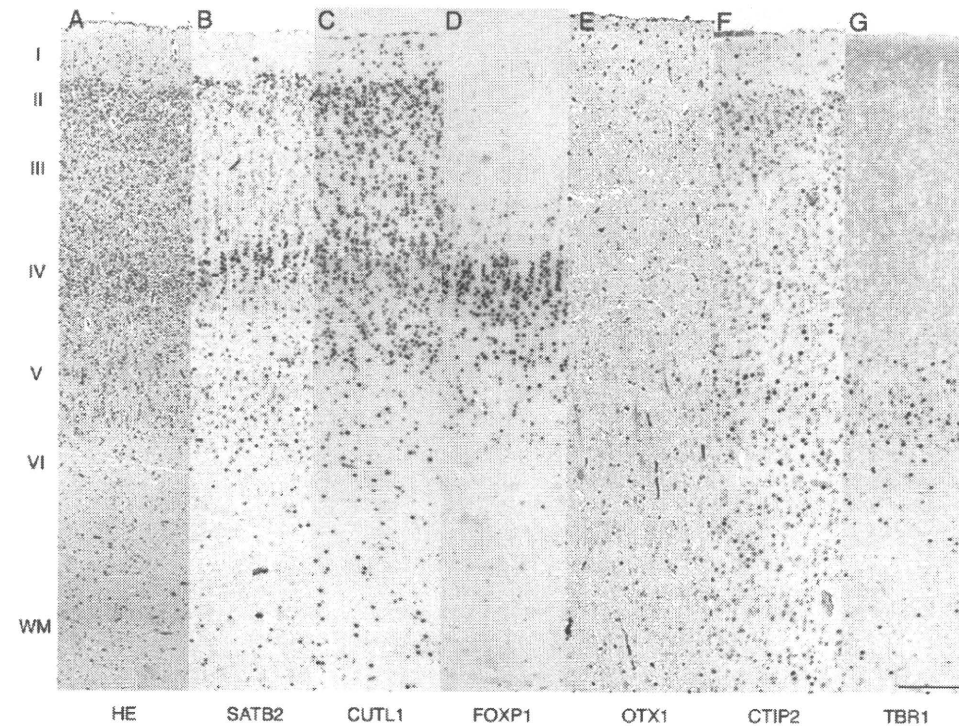


Figure 3. Layer-specific marker expression of the neocortex at 37 GWs. Expression of SATB2, CUTL1, FOXP1, OTX1, CTIP2, and TBR1 has a pattern similar to those at 29 GWs. OTX1 disappears in upper layer of neocortex (E). A, HE; B-G, SATB2, CUTL1, FOXP1, OTX1, CTIP2, and TBR1 immunohistochemistry, respectively. Scale bar: 100 μ m.

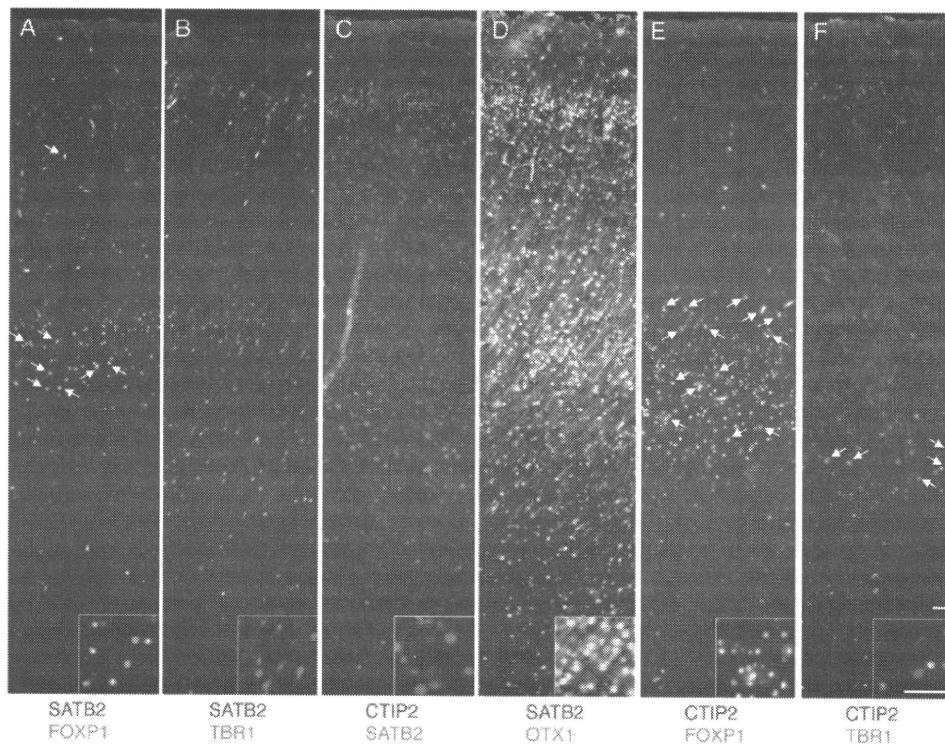


Figure 4. Immunofluorescence of layer-specific marker of neocortex at 29 GWs. FOXP1-immunopositive cells partially have SATB2 (merged color: arrows) in layers II-III and IV-V (A) and CTIP2 (merged color: arrows) in layers IV-VI (E). No double-positive cells for SATB2 and CTIP2 are scattered throughout all layers (C). No TBR1+ and SATB2+ cells are observed in layers V and VI (B), but a few TBR1+ and CTIP2+ cells are seen in layers V and VI (F). Many merged cells with SATB2 (red) and OTX1 (green) are diffusely demonstrated, predominantly in layers II and V (D). A, SATB2 (red) and FOXP1 (green) double fluorescence; B, SATB2 (red) and TBR1 (green); C, CTIP2 (red) and SATB2 (green); D, SATB2 (red) and OTX1 (green); E, CTIP2 (red) and FOXP1 (green); F, CTIP2 (red), and TBR1 (green). Scale bars: 20 μ m.

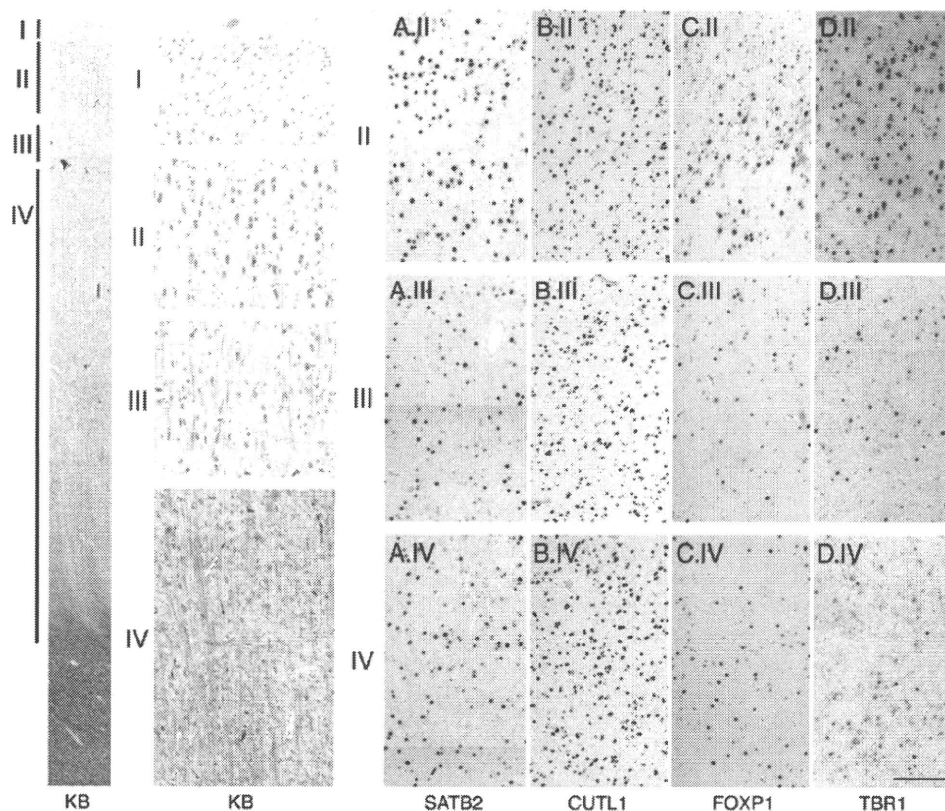


Figure 5. Layer-specific marker expression of the neocortex of 1-year-old patient with Miller-Dieker syndrome. Typical 4-layer pattern is shown. (A) SATB2, CUTL1, FOXP1, and TBR1 are diffusely expressed in layers II, III, and IV. Especially, TBR1-immunopositive cells locate in layer II (E). Enlargement of layer II shows A.II, B.II, C.II, and D.II. Enlargement of layer III shows A.III, B.III, C.III, and D.III. Enlargement of layer IV shows A.IV, B.IV, C.IV, and D.IV. Gross histology shows with KB staining. A.II, A.III, and A.IV, SATB2 in layers II, III, and IV; B.II, B.III, and B.IV, CUTL1; C.II, C.III, and C.IV, FOXP1; D.II, D.III, and D.IV, TBR1, respectively. Scale bar: 100 μ m.

neurons (layer II), and a deep layer (layer III) (Fig. 6A). SATB2+ and CUTL1+ cells located in the intermediate layer and upper region of the deep layer (Fig. 6B,C). FOXP1+ cells and TBR1+ cells were also distributed in layer II and III (Fig. 6D,E). These labeled cells in the deep intermediate layer were large and dense but small and sparse in the upper region of the intermediate layer. Also, in the molecular layer, FOXP1+ and TBR1+ cells were few. No CTIP2+ and OTX1+ cells were observed in either malformed brain.

Usually, FCMD cerebral cortices show type II lissencephaly with cobblestone cortex. The cerebral cortices of FCMD fetus already revealed typical cobblestone lissencephaly (Fig. 7A). Neurons of the fetal neocortex migrated over the glia limitans. SATB2+, CUTL1+, FOXP1+, CTIP2+, and TBR1+ cells were dense above the glia limitans and sparse below it (Fig. 7B-D), and TBR1+ cells were distributed predominantly below the glia limitans (Fig. 7E). However, no markers were detected in specimens from postnatal FCMD brains (data not shown).

The layer-specific marker expression pattern of 3 types of lissencephalies was summarized in Supplementary Figure 2.

Discussion

Very little is known about the molecular mechanism of human neocortex layer formation. Here, we presented new knowledge regarding the layer-specific marker expression in fetus de-

velopment. Recent neuronal developmental studies have introduced some molecules as layer-specific markers. Among them, *Satb2*, *Cutl1*, *Foxp1*, *Otx1*, *Ctip2*, and *Tbr1* are well-known transcriptional factors and highly conserved. The facts that SATB2 was relatively limited to layers II and IV of human fetus cortex and that *Cutl1* was not known in human but was expressed in layers II-IV evidenced the same expression patterns of these molecules in rodent study (Nieto et al. 2004; Britanova et al. 2008). The migration pattern of callosal projection neurons may be the same as that in the mouse. FOXP1+ cells located in deep layers or layers IV-V before 30 GW and in layers IV-VI before birth. TBR1+ cells located in layers V-VI in the fetal period. FOXP1+ and TBR1+ cell localization in layers IV and V was similar to those in a previous human study (Sheen et al. 2006). However, TBR1+ cells were located beneath FOXP1+ cells but not colocalized. The restricted distribution of CTIP2+ cells in layer V may reflect the corticospinal projection formation, as indicated by mouse *ctip2* analysis (Arlotta et al. 2005). Interestingly, SATB2+ cells were located in the upper region of layer IV and FOXP1+ cells in the lower region of the same layer. This different localization indicates completely different neural functions between SATB2 and FOXP1, although the FOXP1 function in neocortex is unknown.

In mouse neocortex, *Otx1*+, *Tbr1*+, *Ctip2*+, *Foxp1*+, *Cutl1*+, and *Satb2*+ neurons are born around embryonic day 12.5, 10.0,

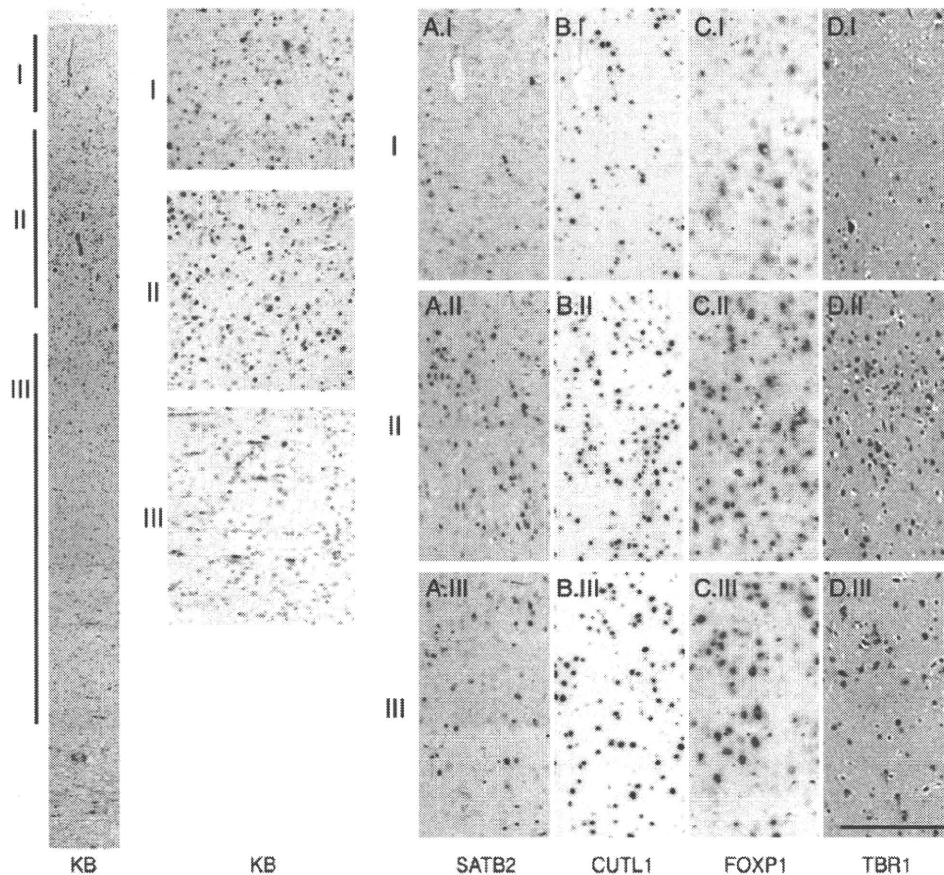


Figure 6. Layer-specific marker expression of the neocortex of 10-month-old boy with XLAG. Neocortex shows a thin 3-layer pattern. SATB2-, CUTL1-, FOXP1-, and TBR1-immunopositive cells locate diffusely (A–D). Gross histology shows with KB staining. A.I, A.II, and A.III, SATB2 in layers I, II, and III; B.I, B.II, and B.III, CUTL1; C.I, C.II, and C.III, FOXP1; D.I, D.II, and D.III, TBR1, respectively. Scale bar: 100 μ m.

12.0, 14.5, 13.0, and 13.5, respectively (Simeone et al. 1993; Bulfone et al. 1995; Hevner et al. 2001; Ferland et al. 2003; Leid et al. 2004; Nieto et al. 2004; Arlotta et al. 2005; Britanova et al. 2005). These labeling neurons originate from progenitor cells residing in the ventricular zone (VZ) and the subventricular zone (SVZ) of early developing brain. Early progenitor cells in VZ produce deep layer neurons expressing Ctip2. On the contrary, late progenitor cells in SVZ form upper layers, expressing Cutl1 (Nieto et al. 2004). The previous data that Satb2-null mice show loss of Cutl1+ cells in the superficial layers (Alcamo et al. 2008) suggest the profound molecular relationship of Satb2 and Cutl1. Satb2+ cells directly contribute to the formation of a callosal projection of the bilateral neocortical connection (Alcamo et al. 2008), while Ctip2+ cells contribute to the formation of a corticospinal projection forming a long pathway between the neocortex and anterior horn of the spinal cord (Arlotta et al. 2005). Interestingly, the expression patterns of SATB2 and CTIP2 in human neocortex mimicked those of rodent, and SATB2+ cells were also found in part of layer V. Although SATB2+ cells and CTIP2+ cells were in layer V, these double-marked cells were not observable. This may indicate these cells have different functions. From rodent study, 2 major projection neurons, callosal and subcortical, are formed by Satb2 and Ctip2 interaction (Leone et al. 2008), which may be at work in the human fetal

neocortex. The finding of no double-labeled cells with CTIP2 and SATB2 in human neocortex is compatible with the rodent data (Leone et al. 2008). Otx1 in mouse brain also expresses in layer V and contributes to the formation of the corticospinal projection (Frantz et al. 1994; Weimann et al. 1999). CTIP2+/OTX1+ cells may be closely related to the forming of the corticospinal projection. Interestingly, we found many SATB2+/OTX1+ cells in layer V. OTX1 may play an essential role in the specification of both callosal and corticospinal projection neurons, although the detailed interaction between OTX1 and CTIP2 remains unknown. Moreover, FOXP1+ cells expressed SATB2 and CTIP2 in layer V. It is unknown whether a relationship exists between Foxp1 and Satb2 or Foxp1 and Ctip2, although Ctip2 is known to colocalize with Foxp1 in mouse striatum (Arlotta et al. 2008). FOXP1 may also contribute callosal and corticospinal projection neurons. FOXP1 disappeared earlier than OTX1 (Figs 2 and 3 and Supplementary Figure 1). FOXP1 could strongly control forming corticospinal projection. Tbr1+ cells derived from the earliest progenitor cells locate in layer VI (Hevner et al. 2003) and contribute to the development of corticothalamic projection neurons (Hevner et al. 2001, 2002; Guillemot et al. 2006; Leone et al. 2008). In our data, the TBR1+ cells that expressed CTIP2 in layer VI may form corticothalamic projections, as in rodent studies.

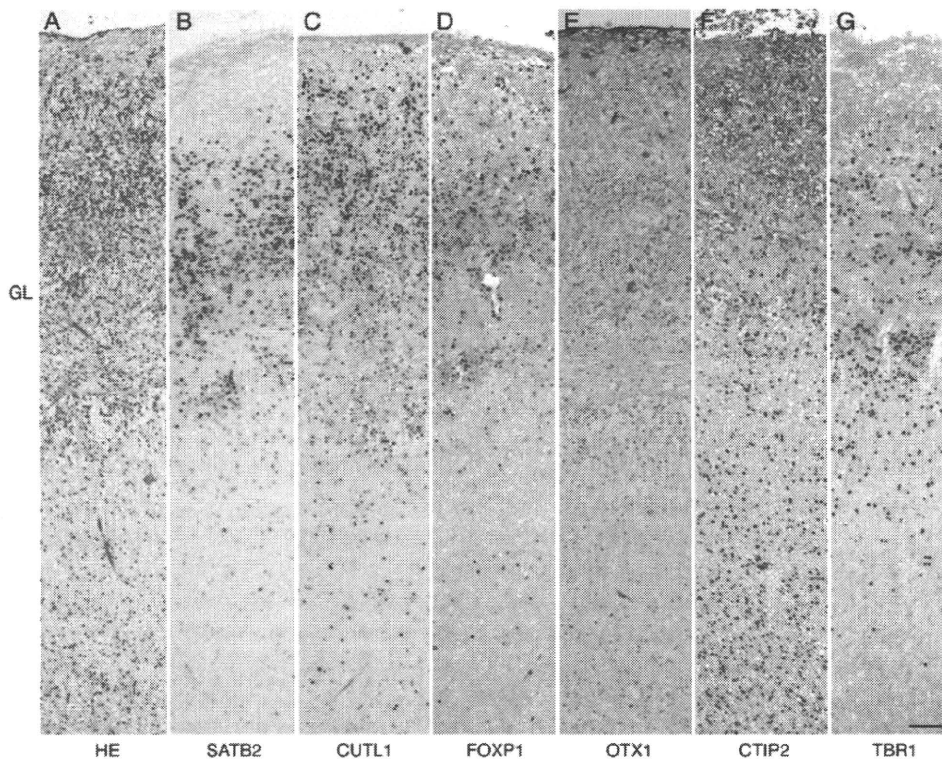


Figure 7. Layer-specific marker expression of the neocortex of 19-GW fetus with FCMD. Neocortex shows typical cobblestone lissencephaly feature. Many SATB2-, CUTL1-, FOXP1-, OTX1-, CTIP2-, and TBR1-immunopositive cells migrate over the glia limitans (B-G), while some labeled cells locate under it. GL, glia limitans; A, HE; B-G, SATB2, CUTL1, FOXP1, OTX1, CTIP2, and TBR1 immunohistochemistry, respectively. Scale bar: 100 μ m.

On the other hand, malformed neocortices revealed unique distributions of the layer-specific markers. In MDS, due to deletion of 17p13.3 with LIS1 gene, it has been thought that neurons of the superficial layer are neuronal components of the fundamental deep layers, and neurons of the deep layers consist of neuronal components of layers II-IV in the normal neocortex (Ferrer et al. 1987). Also, MDS neocortical lamination was found to have an inverted organization (Viot et al. 2004). However, recently the neocortex of 33 GW MDS has reportedly demonstrated FOXP1+ cell in the deep layers or TBR1+ cells in the first 3 layers (Sheen et al. 2006). MDS neocortical lamination was concluded to be preserved and noninverted. Our MDS findings supported noninverted lamination because of the diffuse expression pattern of all layer-specific markers. XLAG, caused by loss of function mutations of ARX gene concerned with differentiation and migration of γ -aminobutyric acidergic interneurons, shows a 3-layer lissencephalic neocortex (Kitamura et al. 2002; Bonneau et al. 2002; Cobos et al. 2005; Forman et al. 2005). Although ARX-null mice exhibit nearly normal layer formation of the cerebral cortex (Kitamura et al. 2002), the human XLAG neocortex was reported to consist of 3 layers with uniform pyramidal neurons (Bonneau et al. 2002; Okazaki et al. 2008). From our observation of layer-specific markers in layers II and III, XLAG might also be a random migration pattern. In human brain, ARX involves migration of not only interneurons but also projection neurons (Okazaki et al. 2008). XLAG neocortex may have an abnormal interneuron migration pattern, although in the present study this could not be demonstrated. Interestingly, our postnatal

patients with MDS and XLAG revealed persistent expression of these layer-specific markers, which was not found in the normal neocortex. This suggests that MDS or XLAG neurons arrest in the premature or undifferentiated stage.

Further investigation is needed to determine why these layer-specific markers are expressed in postnatal brains, and the nature of their molecular function. Moreover, we investigated neocortices of typical type II lissencephaly, FCMD. Various-sized and/or disoriented neurons were widely scattered in the neocortex. In FCMD fetal brain, the layer-specific markers diffusely expressed over and under glia limitans (Fig. 7). Obviously, the FCMD fetal neocortex had completely lost its layer formation. The layer-formation pattern of WWS fetus presents the same result as ours (Hevner 2007). This type II lissencephaly, cobblestone lissencephaly, may commonly have this pathological construction. Postnatal FCMD demonstrated no expression of the layer-specific markers and was different from MDS and XLAG. Neuronal maturation of FCMD neocortex may be more advanced than other types of lissencephalies. This leads us to conclude that FCMD patients have a relatively low incidence of epilepsy and some cases are mild (Guerrini and Filippi 2005; Spalice et al. 2009).

Our study suggests that the laminar formation pattern of human and rodent neocortices is fundamentally the same. One of the characteristics of the human neocortex is its gyration, which is 1000-fold in the neocortical surface area between human and rodent (Bystron et al. 2006; Rakic 2009). It is thought that not only the number of neuronal progenitors but also the number of radial glial cells in human brain is much

larger than in the rodent. As a result, the human neocortex must fold and form gyrations. However, in case of abnormal expression of migration- or proliferation-related genes or environments such as trauma and infection, the number of neuronal progenitor cells, and radial glial cells may serve to reduce and influence the migration pattern.

We may conclude that the neocortex of lissencephalies is formed by a unique type of neuronal migration. The late-birth cells in MDS may migrate randomly but not the early-birth cells. In XLAG, SATB2+, and TBR1+ cells distribute in the relatively deep layers, but CUTL1+ and FOXP1+ cells may follow a random migration pattern. FCMD shows the most random pattern. We must seek to understand the mechanism behind these differences. The molecular mechanism of neuronal movement is well known. Lis-1 or Dcx is a modulator of radial migration and contributes to layer formation (Hirotsumi et al. 1998; Meyer et al. 2002; Bai et al. 2003). In human layer formation, various projection neurons originate from VZ or SVZ and migrate radially depending on the time of cell birth. In interneuron development, Cutl1 and Cutl2 contribute to Reln expression and control the number of the interneuron subpopulation (Cubelos et al. 2008). However, little is known about interaction between the layer-specific markers (transcription factors) and neuron kinetic factors including Lis-1, Dcx and Reln. Further study is warranted to obtain more information in this regard.

Supplementary Material

Supplementary material can be found at: <http://www.cercor.oxfordjournals.org/>.

Funding

Ministry of Health, Labor and Welfare of Japan (Intramural Research Grant [21B-5] for Neurological and Psychiatric Disorders of NCNP, and Research on Intractable Diseases 21-110 and 22-133 to M.I.).

Notes

We thank Drs M. Morikawa, Tokyo Metropolitan Kiyose Children's Hospital, B. Akikusa, Matsudo Municipal Hospital, and H. Horie, Chiba Children's Hospital, for advice on the pathology in this study, and Dr K. Kitamura, National Center of Neurology and Psychiatry, for helpful comments on the manuscript. We are also indebted to Mrs Y. Shono, Tokyo Metropolitan Hachioji Hospital, and Mr S. Kumagai, National Center of Neurology and Psychiatry, for technical assistance. *Conflict of Interest:* None declared.

References

Alcama EA, Chirivella L, Dautzenberg M, Dobrova G, Fariñas J, Grosschedl R, McConnell SK. 2008. Satb2 regulates callosal projection neuron identity in the developing cerebral cortex. *Neuron*. 57:364-377.

Arlotta P, Molyneaux BJ, Chen J, Inoue J, Kominami R, Macklis JD. 2005. Neuronal subtype-specific genes that control corticospinal motor neuron development in vivo. *Neuron*. 45:207-221.

Arlotta P, Molyneaux BJ, Jabaudon D, Yoshida Y, Macklis JD. 2008. Ctip2 controls the differentiation of medium spiny neurons and establishment of the cellular architecture of the striatum. *J Neurosci*. 28:622-632.

Assadi AH, Zhang G, Beffert U, McNeil RS, Renfro AL, Niu S, Quattrocchi CC, Antalfy BA, Sheldon M, Armstrong DD, et al. 2003. Interaction of reelin signaling and Lis1 in brain development. *Nat Genet*. 35:270-276.

Bai J, Ramos RL, Ackman JB, Thomas AM, Lee RV, LoTurco JJ. 2003. RNAi reveals doublecortin is required for radial migration in rat neocortex. *Nat Neurosci*. 6:1277-1283.

Bonneau D, Toutain A, Laguërière A, Marret S, Saugier-Verber P, Barthez MA, Radi S, Biran-Mucignat V, Rodriguez D, Gélot A. 2002. X-linked lissencephaly with absent corpus callosum and ambiguous genitalia (XLAG): clinical, magnetic resonance imaging, and neuropathological findings. *Ann Neurol*. 51:340-349.

Britanova O, Akopov S, Lukyanov S, Gruss P, Tarabykin V. 2005. Novel transcription factor Satb2 interacts with matrix attachment region DNA elements in a tissue-specific manner and demonstrates cell-type-dependent expression in the developing mouse CNS. *Eur J Neurosci*. 21:658-668.

Britanova O, de Juan Romero C, Cheung A, Kwan KY, Schwark M, Gyorgy A, Vogel T, Akopov S, Mitkovski M, Agoston D, et al. 2008. Satb2 is a postmitotic determinant for upper-layer neuron specification in the neocortex. *Neuron*. 57:378-392.

Bulfone A, Smiga SM, Shimamura K, Peterson A, Puelles L, Rubenstein JL. 1995. T-brain-1: a homolog of Brachyury whose expression defines molecularly distinct domains within the cerebral cortex. *Neuron*. 15:63-78.

Bystron I, Rakic P, Molnar Z, Blackmore C. 2006. The first neurons of the human cerebral cortex. *Nat Neurosci*. 9:880-885.

Cobos I, Broccoli V, Rubenstein JL. 2005. The vertebrate ortholog of Aristaless is regulated by Dlx genes in the developing forebrain. *J Comp Neurol*. 483:292-303.

Crome L. 1956. Pachygyria. *J Pathol Bacteriol*. 71:335-352.

Cubelos B, Sebastian-Serrano A, Kim S, Redondo JM, Walsh C, Nieto M. 2008. Cux-1 and cux-2 control the development of reelin expressing cortical interneurons. *Dev Neurobiol*. 68:917-925.

De Rouvoit CL, Goffinet AM. 2001. Neuronal migration. *Mech Dev*. 105:47-56.

Dobyns WB, Berry-Kravis E, Havernick NJ, Holden KR, Viskochil D. 1999. X-linked lissencephaly with absent corpus callosum and ambiguous genitalia. *Am J Med Genet*. 86:331-337.

Ferland RJ, Cherry TJ, Preware PO, Morrissy EE, Walsh CA. 2003. Characterization of Foxp2 and Foxp1 mRNA and protein in the developing and mature brain. *J Comp Neurol*. 460:266-279.

Ferrer I, Fábregues I, Condom E. 1987. A Golgi study of the sixth layer of the cerebral cortex. III. Neuronal changes during normal and abnormal cortical folding. *J Anat*. 152:71-82.

Forman MS, Sguler W, Dobyns WB, Golden JA. 2005. Genotypically defined lissencephalies show distinct pathologies. *J Neuropathol Exp Neurol*. 64:847-857.

Frantz GD, Weimann JM, Levin ME, McConnell SK. 1994. Otx1 and Otx2 define layers and regions in developing cerebral cortex and cerebellum. *J Neurosci*. 14:5725-5740.

Guerrini R, Filippi T. 2005. Neuronal migration disorders, genetics, and epileptogenesis. *J Child Neurol*. 20:287-299.

Guillemot F, Molnar Z, Takabykin V, Stoykova A. 2006. Molecular mechanisms of cortical differentiation. *Eur J Neurosci*. 23:857-868.

Hevner RF. 2007. Layer-specific markers as probes for neuron type identity in human neocortex and malformations of cortical development. *J Neuropathol Exp Neurol*. 66:101-109.

Hevner RF, Miyashita-Lin E, Rubenstein JLR. 2002. Cortical and thalamic axon pathfinding defects in Tbr1, Gbx2, and Pax6 mutant mice: evidence that cortical and thalamic axons interact and guide each other. *J Comp Neurol*. 447:8-17.

Hevner RF, Neogi T, Englund C, Daza RAM, Fink A. 2003. Cajal-Retius cells in the mouse: transcription factors, neurotransmitters, and birthdays suggest a pallial origin. *Brain Res Dev Brain Res*. 141:39-53.

Hevner RF, Shi L, Justice N, Hsueh Y, Sheng M, Smiga S, Bulfone A, Goffinet AM, Campagnoni AT, Rubenstein JL. 2001. Tbr1 regulates differentiation of the preplate and layer 6. *Neuron*. 29:353-366.

Hirotsumi S, Fleck MW, Gambello MJ, Bix GJ, Chen A, Clark GD, Ledbetter DH, McBain CJ, Wynshaw-Boris A. 1998. Graded reduction of Pafah1b1 (Lis1) activity results in neuronal migration defects and early embryonic lethality. *Nat Genet*. 19:333-339.

Kitamura K, Yanazawa M, Sugiyama N, Miura H, Izuka-Kogo A, Kusaka M, Omichi K, Suzuki R, Kato-Fukui Y, Kamiyama K, et al.

2002. Mutation of ARX causes abnormal development of forebrain and testes in mice and X-linked lissencephaly with abnormal genitalia in humans. *Nat Genet.* 32:359-369.
- Leid M, Ishmael JE, Avram D, Shepherd D, Fraulob V, Dollé P. 2004. CTIP1 and CTIP2 are differentially expressed during mouse embryogenesis. *Gene Expr Patterns.* 4:733-739.
- Leone DP, Srinivasan K, Chen B, Alcamo E, McConnell SK. 2008. The determination of projection neuron identity in the developing cerebral cortex. *Curr Opin Neurobiol.* 18:28-35.
- Meyer G, Perez-Garcia CG, Gleeson JG. 2002. Selective expression of doublecortin and LIS1 in developing human cortex suggests unique modes of neuronal movement. *Cereb Cortex.* 12:1225-1236.
- Michele DE, Barresi R, Kanagawa M, Saito F, Cohn RD, Satz JS, Dollar J, Nishino I, Kelley RI, Somer H, et al. 2002. Post-translational disruption of dystroglycan-ligand interactions in congenital muscular dystrophies. *Nature.* 418:417-422.
- Mochida GH, Walsh CA. 2004. Genetic basis of developmental malformations of the cerebral cortex. *Arch Neurol.* 61:637-640.
- Molyneaux BJ, Arlotta P, Menezes JRL, Macklis JD. 2007. Neuronal subtype specification in the cerebral cortex. *Nat Rev Neurosci.* 8:427-437.
- Nieto M, Monuki ES, Tang H, Imitola J, Haubst N, Khoury SJ, Cunningham J, Gotz M, Walsh CA. 2004. Expression of Cux-1 and Cux-2 in the subventricular zone and upper layers II-IV of the cerebral cortex. *J Comp Neurol.* 479:168-180.
- Okazaki S, Ohsawa M, Kuki I, Kawawaki H, Koriyama T, Ri S, Ichiba H, Hai E, Inoue T, Nakamura H, et al. 2008. Aristaless-related homeobox gene disruption leads to abnormal distribution of GABAergic interneurons in human neocortex: evidence based on a case of X-linked lissencephaly with abnormal genitalia (XLAG). *Acta Neuropathol.* 116:453-462.
- Olson EC, Walsh CA. 2002. Smooth, rough and upside-down neocortical development. *Curr Opin Genet Dev.* 12:320-327.
- Rakic P. 2009. Evolution of the neocortex: a perspective from developmental biology. *Nat Rev Neurosci.* 10:724-735.
- Reiner O, Sapir T. 2009. Polarity regulation in migrating neurons in the cortex. *Mol Neurobiol.* 40:1-14.
- Sheen VL, Ferland BJ, Neal J, Harney M, Hill RS, Banham A, Brown P, Chenn A, Corbo J, Hecht J, et al. 2006. Neocortical neuronal arrangement in Müller Dieker syndrome. *Acta Neuropathol.* 111:489-496.
- Simeone A, Acampora D, Mallamaci A, Stornaiolo A, D'Apice MR, Nigro V, Boncinelli E. 1993. A vertebrate gene related to *orthodenticle* contains a homeodomain of the *bicoid* class and demarcates anterior neuroectoderm in the gastrulating mouse embryo. *EMBO J.* 12:2735-2747.
- Spalice A, Parisi P, Nicita F, Pazzardi G, Del Balzo F, Iannetti. 2009. Neuronal migration disorders: clinical, neuroradiologic and genetic aspects. *Acta Paediatr.* 98:421-433.
- Viot G, Sonigo P, Simon I, Simon-Bouy B, Chadeyron F, Beldjord C, Tantau J, Martinovic J, Esculpavit C, Brunelle F, et al. 2004. Neocortical neuronal arrangement in LIS1 and DCX lissencephaly may be different. *Am J Med Genet A.* 126A:123-128.
- Weimann JM, Zhang YA, Levin ME, Devine WP, Bulet P, McConnell SK. 1999. Cortical neurons require *otx1* for the refinement of exuberant axonal projections to subcortical targets. *Neuron.* 24:819-831.
- Yamamoto T, Kato Y, Kawaguchi M, Shibata N, Kobayashi M. 2004. Expression and localization of fukutin, POMGnT1, and POMT1 in the central nervous system: consideration for functions of fukutin. *Med Electron Microsc.* 37:200-207.

原 著

Mecp2 欠損 Rett 症候群モデルマウスにみられる呼吸の異常と病態変化

和田 崇¹⁾・滝口旗一¹⁾・武内倫子¹⁾・黒木洋祐¹⁾関 信幸¹⁾・高森一乗^{1,2)}・白川哲夫^{1,2)}

要旨：Rett 症候群は主として女兒に発症する疾患で、自閉症状のほか、上下肢の協調運動障害、手もみ様の常同運動、歯ぎしり、息止め発作などを特徴とする。原因遺伝子である MeCP2 (methyl-CpG binding protein 2) が欠損した雄マウス (Mecp2^{-/-}) では、同症候群に類似した無呼吸がみられる。本研究では、Mecp2^{-/-}の無呼吸の特性を明らかにする目的で、全身型プレチスモグラフによって無拘束下で呼吸波形を測定して、野生型雄マウス (wild) と比較した。

Mecp2^{-/-}では、1秒以上続く無呼吸の回数が生後5週でwildと比べ有意に多く、7週で無呼吸の回数はさらに増加した。1日の時間帯で無呼吸の回数に違いがあるかどうかを調べる目的で、明期 (7:00~19:00) のうちの4時間 (11:00~15:00) と暗期 (19:00~7:00) のうちの4時間 (23:00~3:00) で比較したところ、5週齢、7週齢いずれにおいても無呼吸回数は明期に多かった。マウスを恒暗条件下に置き、11:00~15:00の時間帯で無呼吸回数を測定して明暗条件下での計測値と比較したところ、wildでは違いがみられなかったが Mecp2^{-/-}では無呼吸回数が有意に少なかった。これらの結果は、光刺激が Mecp2^{-/-}の呼吸中枢に作用して呼吸リズムの形成になんらかの影響を与えている可能性を示唆している。

以上より、本モデルマウスは、Rett 症候群における無呼吸の病態の解明に有用と考えられた。

Key words : Rett syndrome, MeCP2, Apnea, Mouse model

摘 言

Rett 症候群は約1万人に1人の頻度で主に女兒に発症する X 連鎖優性遺伝病である。1966年に小児神経科医 Andreas Rett によって初めて報告され¹⁾、1983年の Hagberg らの報告²⁾によって広く知られるようになった。いずれの報告においても、本症は乳児期に正常な発育を示すが、1歳を過ぎて発症した後は、四肢協調運動の障害や上肢の常同運動など特徴的な症状を呈すること、および退行性の経過をたどることが記されている。

その後の研究により、本症は X 染色体上に存在する MeCP2 (methyl-CpG binding protein 2) の遺伝子変異が発症に直接関与していることが明らかにされた^{3,4)}。Rett 症候群患者は自閉症状、てんかん、重度の精神遅滞、側湾、失調性歩行、睡眠リズムの異常、異常な呼吸パターン、摂食機能障害、歯ぎしり、特有の常同運動 (指打ち、手擦り、手打ちなど)、自律神経障害、

などを特徴とする¹⁻⁷⁾。また呼吸パターンの異常は多くの場合、過呼吸・無呼吸を断続的に繰り返すものが多いといわれている。これらの呼吸異常は睡眠時には出現しないとされており、日中、特に精神緊張時に顕著になることが報告されている⁸⁾。

本症の原因遺伝子 MeCP2 が同定されたのち、そのノックアウトマウスが作成された⁹⁾。MeCP2 をもたない雄マウス (Mecp2^{-/-}) では、出生時には異常がみられないものの、生後3~5週頃からヒトと同じような症状が出現し、通常10週以内に死亡する⁹⁾。

本研究では、Mecp2^{-/-}においておおむね生後5週以降に顕在化することが示されている無呼吸の病態について検討する目的で、全身型プレチスモグラフを用いて無拘束下で呼吸波形の測定を行い、呼吸の特性について解析した。また現在のところ、Rett 症候群にみられる息ごらえ発作がなぜ覚醒時のみに出現するのかについて全く不明であることから、Mecp2^{-/-}の呼吸波形を明期および暗期でそれぞれ4時間ずつ記録し解析を行った。

材料ならびに方法

1. 実験動物および飼育条件

Mecp2 ヘテロ欠損雌マウス (B6 ; 129 P2-Mecp2^{tm1.1Bivd}/J, STOCK # 003890 ; Jackson Labora-

¹⁾日本大学歯学部小児歯科学講座

(主任：白川哲夫教授)

²⁾日本大学歯学部総合歯学研究所顎口腔機能研究部門

(原稿受付日：平成22年6月15日)

(原稿受理日：平成22年9月6日)

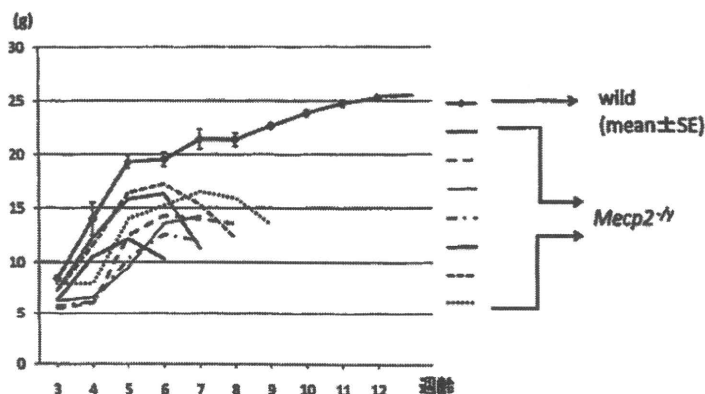


図1 *Mecp2*^{-/-}の体重変化と生存期間

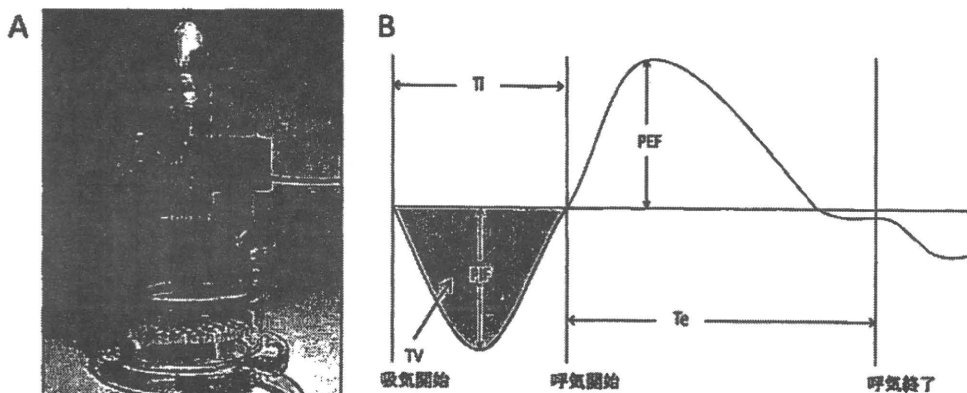


図2

A 全身型プレチスモグラフのチャンパー
B 呼吸波形についての計測パラメータ

tory, Bar Harbor, Maine, USA) ならびに C57BL/6J 野生型雄マウス (オリエンタル酵母工業, 東京) を購入後, 本学動物実験施設にて飼育し, 両者を交配することで *Mecp2*^{-/-}を得た. コントロールとして, C57BL/6J の雄マウス (wild) を用いた. 食餌にはマウス・ラット・ハムスター用飼料 MF 飼育用 (オリエンタル酵母工業) を用いた.

飼育環境は明期 7:00~19:00, 暗期 19:00~7:00, 室温 24±1°C, 湿度 50±5%とした. 出産後, 飼育ケージ内で母親に授乳させ, 生後 21 日に母仔を分離した. 離乳後は個体ごとに分離して飼育し, それぞれの仔マウスについて 1 週間ごとに体重を計測した. 飼育室の照度は, 蓋を外した状態での飼育ケージの床部での測定で 40~50 lux であった.

MeCP2タンパクを全く作ることができない *Mecp2*^{-/-}では, 出生時には異常がみられないものの, 生後 3~5 週頃からヒトに類似した無呼吸や運動の異常

が出現し, 症状が徐々に進行して通常 10 週以内に死亡する⁹⁾. 予備実験において生後 7 週以降で死亡率が増加し, 生後 8 週以降では呼吸の測定期間中に死亡する個体がみられたことから (図 1), 本研究では 5 週齢および 7 週齢の *Mecp2*^{-/-}を測定対象とした.

なお, 本研究は日本大学歯学部実験動物委員会の承認を得て実施し, 実験動物の取扱いは同委員会の指針に従って行った (承認番号 18-7 2006 歯 007-1, 007-2).

2. 呼吸測定

週齢が等しい *Mecp2*^{-/-}と wild で呼吸を測定した. マウスを無麻酔の状態で一匹ずつ全身型プレチスモグラフ (PLY 4211; Buxco Electronics, 大阪) のチャンパー内に入れ (図 2 A), 圧トランスデューサーと増幅器により, 呼吸に伴うチャンパー内の気流変化を検出することにより呼吸波形を連続的に測定・記録した. 記録時間は, 暗期の 23:00~3:00 (Dark) および明期の

11:00~15:00 (Light) とし、それぞれ測定開始の4時間前にマウスをチャンバーに入れて測定環境に馴化させたのちデータを記録した。チャンバー内の照度は、床部での測定で10 lux になるよう調節した。

プレチスモグラフによる測定を生後5週と7週で行い、1秒以上の無呼吸の発生回数 (Apnea Counts/4 hr)、呼吸頻度 (Breath/min)、一回換気量 (Tidal Volume: TV)、吸気時間 (Inspiratory Time: Ti)、呼気時間 (Expiratory Time: Te)、最大吸気流量 (Peak Inspiratory Flow: PIF)、最大呼気流量 (Peak Expiratory Flow: PEF) について解析を行った (図2 B)。

また、無呼吸に対する明期の光の影響を検討するため、7週齢の *Mecp2*^{-/-} と wild について、19:00 から恒暗条件にして翌日の11:00~15:00 (Dark 2) に呼吸の測定を行い、無呼吸回数について解析を行った。

3. 統計処理方法

統計学的検定には分散分析を用いた。反復測定を含むデータの統計処理には二元配置分散分析を用い、群間に対応のない場合には一元配置分散分析を用いた。また群間比較には Bonferroni 法を用いた。p 値が0.05 未満であるときに有意差ありとした。

結 果

1. 無呼吸回数

図3 A に *Mecp2*^{-/-} ならびに wild から記録した呼吸波形を示す。wild の安静時の呼吸波形はきわめて安定していた。*Mecp2*^{-/-} では、通常は wild に類似した呼吸波形を示したが、安静時であっても図に示すような無呼吸がしばしば出現した。

Mecp2^{-/-} と wild の無呼吸回数の比較では、*Mecp2*^{-/-} で回数が有意に多かった。*Mecp2*^{-/-} の無呼吸回数は、5週齢と比較して7週齢で増加し (図3 B) (5週 wild: 947±102, *Mecp2*^{-/-}: 2,976±203; 7週 wild: 709±61, *Mecp2*^{-/-}: 4,817±325)、いずれの週齢でも暗期に比べ明期で有意に多かった (図3 C) (5週 Dark-wild: 425±54, *Mecp2*^{-/-}: 1,227±115; 5週 Light-wild: 522±60, *Mecp2*^{-/-}: 1,750±312; 7週 Dark-wild: 311±30, *Mecp2*^{-/-}: 1,869±184; 7週 Light-wild: 398±36, *Mecp2*^{-/-}: 2,948±174) (wild: n=8, *Mecp2*^{-/-}: n=7)。明期で無呼吸の回数が増加した理由として、飼育室の光環境が関与している可能性が考えられたため、恒暗条件下で呼吸波形を測定したところ、*Mecp2*^{-/-} の Dark 2 での無呼吸回数は、明暗条件下の Light と比較して有意に少なかった (図3

D) (Dark 2-*Mecp2*^{-/-}: 1,876±287, n=7)。一方、wild では *Mecp2*^{-/-} でみられた無呼吸についての光環境の影響は認められなかった (Dark 2-wild: 406±50, n=8)。

2. 呼吸頻度

5週齢、7週齢ともに wild に比べ *Mecp2*^{-/-} で呼吸頻度が有意に低かった。また明期と暗期の比較では、*Mecp2*^{-/-} ならびに wild ともに明期で呼吸頻度が低かった (図4 A)。

3. 一回換気量

5週齢、7週齢ともに *Mecp2*^{-/-} は wild に比べて有意に低い値を示した。また明期と暗期の比較では、*Mecp2*^{-/-} ならびに wild ともに明期のほうが有意に低かった (図4 B)。

4. 吸気時間、呼気時間

吸気時間について5週齢では *Mecp2*^{-/-} と wild で差がみられなかったが、7週齢では wild に比べ *Mecp2*^{-/-} が有意に長かった。一方、呼気時間は5週齢、7週齢ともに wild に比べ *Mecp2*^{-/-} が有意に長かった。また吸気時間および呼気時間についての明期と暗期の比較では、5週齢、7週齢ともに明期で有意に長かった (図4 C, D)。

5. 最大吸気流量、最大呼気流量

5週齢、7週齢ともに、いずれの流量についても *Mecp2*^{-/-} は wild に比べて有意に少なかった。また明期と暗期の比較では、5週齢、7週齢ともに明期で有意に少なかった (図4 E, F)。

考 察

呼吸異常は Rett 症候群患者にみられる主要な症状の一つであり、無呼吸に伴って過呼吸がみられることも多く、また息ごらえ発作を呈する場合もある²⁰⁾。このような Rett 症候群の呼吸異常は中枢性であり、呼吸リズムを作り出している中枢あるいはそれを調節する機構になんらかの異常があることが推測されている⁹⁾。しかしながら、現在のところ Rett 症候群患者の中枢でどのような病的変化が生じているのかについての報告は少なく^{10,11)}、実体はほとんど明らかにされていない。

興味深いことは、Rett 症候群患者の覚醒時においてみられる無呼吸発作が、睡眠時にはほとんど出現しないことである¹²⁾。このことは、Rett 症候群において、睡眠覚醒に関わる脳機能あるいは外界の明暗環境が呼吸リ

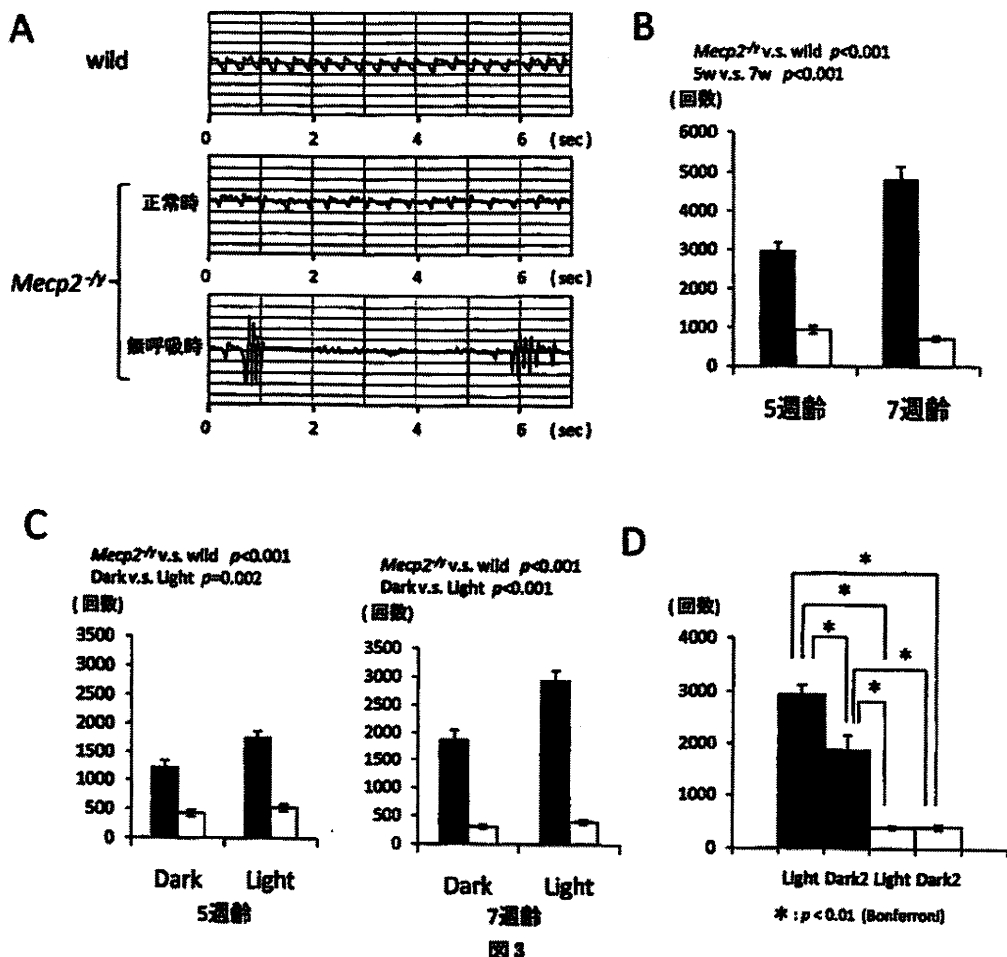


図3

- A 呼吸波形 (7週齢)
- B 無呼吸回数: 明期と暗期の各4時間の合計値の比較
- C 無呼吸回数の明期と暗期の比較
- D 明暗条件下 (Light) と恒暗条件下 (Dark 2) での無呼吸回数の比較
- *Mecp2*^{-1/2} (n=7)
- wild (n=8)

リズム中枢あるいはその調節系に対してなんらかの影響を与えている可能性を示唆する。また、精神の緊張時に無呼吸発作が顕著になることから、睡眠覚醒や明暗条件以外にも呼吸異常を誘発する要因があることが推測され、その有力候補として自律神経系の異常、特に交感神経系と副交感神経系のバランスの乱れが考えられている⁹⁾。本研究では、ヒトに類似した症状を示す *Mecp2*^{-1/2} の呼吸について解析することで、MeCP2の機能異常あるいは欠失が、呼吸調節系にどのような病的変化を惹起しているのかについて調べた。

無呼吸回数が増加する要因として光による直接の影響を考え、マウスを通常の明暗条件ではなく、本来明期で

あるはずの時間帯も暗くする恒暗環境において無呼吸への影響を調べたところ、恒暗条件下の11:00~15:00の時間帯での無呼吸回数について、*Mecp2*^{-1/2}では明暗条件下と比較して有意に無呼吸回数が減少していた。このことは、網膜を介して中枢に伝わった光刺激が、なんらかの経路を通じて呼吸リズムを作り出している中枢に影響を与えていることを示唆している。一方で7週齢のwildでは、そのような光の影響は全く認められなかった。これらのことから、*Mecp2*^{-1/2}については生後7週においても呼吸中枢あるいはその調節系の成熟が不十分か、または機能的に不安定であり、wildマウスに比べて著しく光の影響を受けやすい状態にあると推測された。

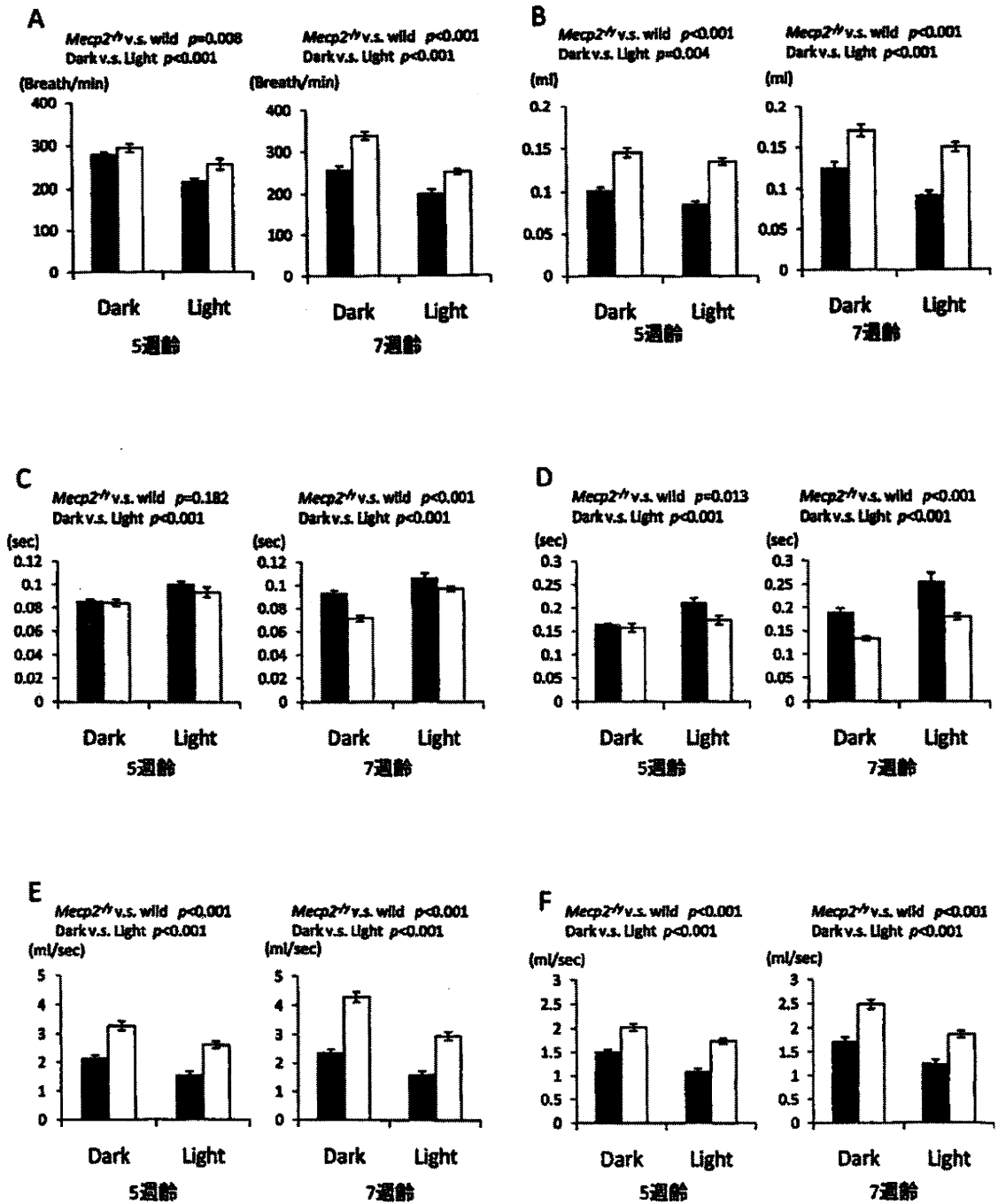


図 4

- A 呼吸頻度
 B 一回換気量
 C 吸気時間
 D 呼気時間
 E 最大吸気流量
 F 最大呼気流量
- *Mecp2^{-/-}* (n=7)
 □ wild (n=8)

呼吸頻度, 一回換気量, 呼気時間, 吸気時間, 最大吸気流量, 最大呼気流量を明期と暗期で比較した結果では, *Mecp2*^{-/-}と wild は同じ傾向を示した。この結果は, サーカディアンリズムを作り出している中枢の基本的な機能が, *Mecp2*^{-/-}においても, 少なくとも生後7週の時点で維持されていることを示している。

Mutohらは光刺激がサーカディアンリズムの中枢である視交叉上核を介してマウスの副交感神経を抑制することを明らかにした¹³⁾。Rett症候群患者において無呼吸発作が精神的緊張時に多くみられるという報告から, 精神的緊張に伴う交感神経の興奮, あるいは副交感神経の抑制が無呼吸の発生に関与していることが示唆されるが, 光刺激がマウスの副交感神経系を抑制することと併せて考えると, *Mecp2*^{-/-}でみられた明期における無呼吸エピソードの増加には, 光刺激による副交感神経の抑制が関与している可能性がある。

ヒトにおいてマウスと同様に光刺激が自律神経系を介してRett症候群の病態に影響を与えているのかどうかは興味深い問題である。一般の障害者と同様に, Rett症候群患者にとっても歯科治療が精神的, 肉体的ストレスになっていることは否定できない。もし, 歯科的ストレスに加えて診療室の比較的明るい環境も無呼吸発作に影響しているならば, 遮光を工夫することで無呼吸の発生を制御できる可能性があり, 今後, 注意深い検証が必要と思われる。

Rett症候群患者の神経学的予後を改善する治療は今のところない。現在のRett症候群患者に対する医療は, 補助医療や対症療法に焦点が当てられている。Rett症候群患者の髄液でオピオイドの上昇が観察され, オピオイド拮抗薬ナルトレキソンの経口投与の効果が研究された。それによると呼吸の不整の減少を認めたが, 薬の鎮静作用の影響もあるため, その効果についてまだ確定的とはいえない¹⁴⁾。なお, ジアゼパムの経口投与により, 無呼吸発作の著明な改善が認められたとの国内の医療機関からの報告があることから¹⁵⁾, 今後, *Mecp2*^{-/-}の呼吸異常について, ジアゼパムなどの薬物の効果を個体レベル, 組織レベルで検討していく必要があると考えられる。

結 論

Mecp2^{-/-}では, 生後5週から7週にかけて無呼吸回数が著しく増加した。無呼吸回数は暗期に比べ明期に多く, 無呼吸の発生に光の刺激が直接関与している可能性が示唆された。

本研究は, 学術フロンティア推進プログラム, 日本学術振興会科学研究費補助金 No.18390551 および No.19659544, ならびに平成21年度日本大学大学院歯学研究科共同研究費および佐藤研究費により実施した。

本研究の成果の一部は第26回日本障害者歯科学会学術大会(2009年10月30日, 名古屋)において発表した。

文 献

- 1) Rett, A.: On a unusual brain atrophy syndrome in hyperammonemia in childhood. *Wien Med. Wochenschr.*, 116: 723-726, 1966.
- 2) Hagberg, B., Aicardi, J., *et al.*: A progressive syndrome of autism, dementia, ataxia, and loss of purposeful hand use in girls: Rett's syndrome: Report of 35 cases. *Ann. Neurol.*, 14: 471-479, 1983.
- 3) Xiang, F., Zhang, Z., *et al.*: Chromosome mapping of Rett syndrome: a likely candidate region on the telomere of Xq. *J. Med. Genet.*, 35: 297-300, 1998.
- 4) Amir, R. E., Van den Veyver, I. B., *et al.*: Rett syndrome is caused by mutations in X-linked MECP2, encoding methyl-CpG-binding protein 2. *Nat. Genet.*, 23: 185-188, 1999.
- 5) Nomura, Y., Segawa, M., *et al.*: Rett syndrome-clinical studies and pathophysiological consideration. *Brain Dev.*, 6: 475-486, 1984.
- 6) Motil, K. J., Schultz, R. J., *et al.*: Oropharyngeal dysfunction and gastroesophageal dysmotility are present in girls and women with Rett syndrome. *J. Pediatr. Gastroenterol. Nutr.*, 29: 31-37, 1999.
- 7) Takamori, K., Kuroshita, R., *et al.*: Electromyographic analysis of bruxism in a patient with Rett syndrome. *Ped. Dent. J.*, 18: 214-217, 2008.
- 8) Guy, J., Hendrich, B., *et al.*: A mouse *Mecp2*-null mutation causes neurological symptoms that mimic Rett syndrome. *Nat. Genet.*, 27: 322-326, 2001.
- 9) Katz, D. M., Dutschmann, M., *et al.*: Breathing disorders in Rett syndrome: progressive neurochemical dysfunction in the respiratory network after birth. *Respir. Physiol. Neurobiol.*, 168: 101-108, 2009.
- 10) Saito, Y., Ito, M., *et al.*: Reduced expression of neuropeptides can be related to respiratory disturbances in Rett syndrome (Suppl.). *Brain Dev.*, 23: 122-126, 2001.
- 11) Itoh, M., Ide, S., *et al.*: Methyl CpG-binding protein 2 (a mutation of which causes Rett syndrome) directly regulates insulin-like growth factor binding protein 3 in mouse and human brains. *J. Neuropathol. Exp. Neurol.*, 66: 117-123, 2007.
- 12) Julu, P. O., Kerr, A. M., *et al.*: Characterisation of breathing and associated central autonomic dysfunction in the Rett disorder. *Arch. Dis. Child.*, 85: 29-37, 2001.

- 13) Mutoh, T., Shibata, S., *et al.* : Melatonin modulates the light-induced sympathoexcitation and vagal suppression with participation of the suprachiasmatic nucleus in mice. *J. Physiol.*, 547 : 317-332, 2003.
- 14) Christodoulou, J. and Ho, G. : MECP2-related disorders. *Gene Reviews*, 2001.
- 15) 栗原まな, 熊谷公明, 他 : Diazepam が無呼吸発作に奏功した Rett 症候群の 6 歳女児例 ポリグラフによる検討. *脳と発達*, 33 : 58-62, 2001.

Breathing Difficulties in a Mouse Model of Rett Syndrome with a *MeCP2*-null Mutation

WADA Takashi¹⁾, TAKIGUCHI Hatakazu¹⁾, TAKEUCHI Michiko¹⁾, KUROKI Yosuke¹⁾, SEKI Nobuyuki¹⁾, TAKAMORI Kazunori^{1,2)} and SHIRAKAWA Tetsuo^{1,2)}

¹⁾Department of Pediatric Dentistry, Nihon University School of Dentistry
(Chief : Prof. SHIRAKAWA Tetsuo)

²⁾Division of Oral and Craniomaxillofacial Research, Dental Research Center,
Nihon University School of Dentistry

Rett syndrome is an X-linked neurodevelopmental disease accompanied by complex, disabling phenotypes, including breathing symptoms. This syndrome mainly affects females, and the patient exhibits stereotyped hand movements, impaired coordination of limbs, grinding of teeth, breath-holding, etc. Because Rett syndrome is caused by mutations in the gene encoding methyl-CpG-binding protein 2 (*MeCP2*), we used *MeCP2*-deficient mice as a model of this syndrome and measured respiratory functions by using whole-body plethysmography.

Heterozygous female mice (B6 ; 129P2-*Mecp2*^{tm1B/mi}/J : Jackson Laboratory) were mated with male C57BL/6J mice in an animal experiment facility at the Nihon University School of Dentistry, and hemizygous *MeCP2*-deficient males (*Mecp2*^{-/-}) were obtained. The breathing pattern of *Mecp2*^{-/-} and male C57BL/6J mice was measured at 5 and 7 weeks of age under a 12 : 12 light-dark cycle (lights on : 7 : 00-19 : 00), and apnea counts, respiration frequency, tidal volume, inspiratory time, expiratory time, peak inspiratory flow, and peak expiratory flow were calculated using software (Buxco Electronics) for analyzing plethysmographic data.

Apnea counts increased with the progress of symptoms at 7 weeks of age in *Mecp2*^{-/-} and the counts were larger during the light phase (11 : 00-15 : 00) than the dark phase (23 : 00-3 : 00). When the animals were placed in constant darkness and the apnea counts during 11 : 00-15 : 00 were compared to the counts obtained under the 12 : 12 light-dark condition, it became apparent that the elimination of light significantly reduced the apnea counts in *Mecp2*^{-/-} but not in male C57BL/6J mice.

These results indicate that the *MeCP2*-null mutation causes progressive breathing difficulties that are more prominent during the light phase than the dark phase. Turning the light off may ameliorate the breathing difficulties in *Mecp2*^{-/-}.



ELSEVIER

Brain & Development xxx (2011) xxx–xxx

BRAIN &
DEVELOPMENTOfficial Journal of
the Japanese Society
of Child Neurology

www.elsevier.com/locate/braindev

Review article

Rett syndrome: The state of clinical and basic research, and future perspectives

Toyojiro Matsuishi^{a,*}, Yushiro Yamashita^a, Tomoyuki Takahashi^b,
Shinichiro Nagamitsu^a

^a Department of Pediatrics and Child Health, Kurume University School of Medicine, Kurume 830-0011, Japan

^b Division of Gene Therapy and Regenerative Medicine, Cognitive and Molecular Research Institute of Brain Diseases, Kurume University, Japan

Received 28 September 2010; accepted 14 December 2010

Abstract

To clarify the pathophysiology of brain and spinal cord impairment in Rett syndrome (RTT), we report on the current status of research on Rett syndrome and review the abnormalities reported in neurotransmitters, neuromodulators and other biological markers in patients with RTT. We have previously investigated the levels of various factors in the blood, plasma, and cerebrospinal fluid (CSF) of RTT patients, including biogenic amines, lactate, melatonin, pyruvate and other citric acid cycle intermediates, substance P, β -endorphin and other neuropeptides, and a neuromodulator of β -phenylethylamine. In addition, we have performed near-infrared spectroscopy of the cerebral cortices in patients with RTT and genetic studies of the methyl-CpG-binding protein 2 (MECP2) in these patients. Taken together, the multiple abnormalities we and other authors have revealed in the various neurotransmitters/neuromodulator systems explain the pervasive effects of Rett syndrome. We also discuss the possible role of plasma ghrelin and present the results of our mouse study of the MECP2-null mutation using ES cells. Finally, we consider the potential for future analyses using our recently developed iPS cell system and discuss the future perspectives for the treatment and management of this disease.

© 2010 The Japanese Society of Child Neurology. Published by Elsevier B.V. All rights reserved.

Keywords: Rett syndrome; Methyl-CpG-binding protein 2; Pathophysiology; Neurotransmitters; Neuromodulators; MECP2-null mutation mouse model

1. Introduction

Rett syndrome (RTT) is a neurodevelopmental disorder characterized by normal early psychomotor development followed by the loss of psychomotor and acquired purposeful hand skills and the onset of stereotyped movement of the hands and gait disturbance [1–4]. The gene was discovered in 1999 and the disease was found to be caused by a mutation of the methyl-CpG-

binding protein 2 [5,6]. However, in many ways this clinically peculiar condition remains a mystery, with no clear correlations between the gene mutation and abnormal biological markers, neuropathology and/or unique clinical symptoms and signs [1–4,6].

RTT is unique among genetic, chromosomal and other developmental disorders because of its usually sporadic occurrence, extreme female gender bias, early normal development and subsequent developmental regression, autonomic dysfunction, stagnation in brain growth and distinctive neuropathology. MECP2 mutations lead to the RTT phenotype in females, and profound congenital encephalopathy in males [7]. Research needs to be directed toward clarifying the link between the MECP2 involvement and the alterations in biological, neurochem-

* Corresponding author. Address: Department of Pediatrics and Child Health, Kurume University School of Medicine, 67 Asahimachi, Kurume City 830-0011, Japan. Tel.: +81 942 31 7565; fax: +81 942 38 1792.

E-mail address: tmatsu@med.kurume-u.ac.jp (T. Matsuishi).

ical, and neurotransmitter/receptor systems, as well as toward developing new therapeutic modalities.

2. Neurotransmitters and biological markers

2.1. Biogenic amines

Nomura and Segawa have suggested that hypoactivity or underdevelopment in the biogenic amines might account for the range of abnormalities found in RTT. Specifically, they suggested that the disease might be associated with impairments in noradrenalin, serotonin, and dopamine based on a series of clinical, electrophysiological and polysomnographic studies. They have proposed that the following points are important in considering the pathophysiology of RTT. First, the characteristic symptoms and signs appear in sequence within a specific age from infancy. The earliest and pathognomonic manifestations of RTT are the autistic tendency and the decreased rate in head growth [8,9]. Their report has led to a proliferation of studies on biogenic amines in the cerebrospinal fluid (CSF) of RTT patients, as well as immunohistochemical studies, receptor studies, and neuroimaging studies. Together, these investigations have suggested that various neurotransmitters, neuromodulators, neurotrophic factors and neuronal markers may be involved in RTT. Zoghbi et al. have reported significant reductions in the levels of homovanillic acid (HVA) and in 3-methoxy-4-hydroxy-phenylethylene glycol (MHPG) in the CSF of children with RTT [10]. However, Perry et al. reported no difference in these levels between RTT patients and controls [11]. Therefore, whether or not CSF biogenic amines are actually altered in RTT remains a matter of controversy. However, a recent report showed that HVA and 5-HIAA were decreased in RTT patients and the MECP2^{null/y} mouse brain [12]. In another study, the biogenic amines dopamine, serotonin, and noradrenalin, and their respective metabolites HVA, 5-hydroxyindoleacetic acid, and MHPG, were measured in tissues from selected brain regions obtained at postmortem from four patients with RTT. A marked reduction in each of these substances was observed and these changes appeared to be age-related [13,14]. In addition, the endogenous levels of dopamine and its metabolites have been shown to be decreased throughout the neocortex and basal ganglia of patients with RTT [15]. Kitt et al. have reported a mild-to-moderate reduction in the number and cell size of the basal forebrain cholinergic neurons in RTT patients compared with controls, which might explain the impaired cognitive function and microcephalus [16].

2.2. β -Phenylethylamine

We have reported decreased β -phenylethylamine (PEA) levels in the CSF of patients with RTT [17].

PEA is an endogenous amine synthesized by decarboxylation of phenylalanine in the dopamine neurons of the nigrostriatal system, and plays an important role in both the dopaminergic and noradrenergic systems. We have also reported reduced levels of PEA in the CSF of patients with Parkinson's disease. The PEA level was also negatively correlated with the severity of the Parkinson's disease [18].

2.3. β -Endorphin, substance P, melatonin

Myer et al. [19] and Budden et al. [20] have reported elevated CSF β -endorphin in RTT. However, elevated β -endorphin was not found in the brain, suggesting that the alteration in β -endorphin may be a secondary change. We have reported that the level of substance P was markedly decreased in the CSF in patients with RTT, and this was considered to play a role in the features of autonomic dysfunction that occur in RTT, including constipation, small and cold feet, progressive limb muscle weakness and muscle atrophy [21]. Substance P is a neurotransmitter or neuromodulator in the peripheral as well as the central nervous system (CNS). Substance P activity is associated with dopaminergic neurons in the substantia nigra and the striatum, the central autonomic nuclei, the dorsal root ganglia, and the peripheral autonomic ganglia [22]. Hedner et al. reported that substance P acted on the respiratory control system by at least two different mechanisms: the bulbo-pontine time setting mechanism, and the inspiratory off-switch mechanism [23]. Deguchi et al. reported that the substance P immunoreactivity was significantly decreased in brain tissues, especially the solitary tract and nucleus, parvocellular and pontine reticular nuclei, and locus coeruleus, with less significant decreases in the substantia nigra, central gray matter of the mid-brain, and other regions. Glial fibrillary acidic protein (GFAP)-positive astrocytes were increased in the areas in which SP immunoreactivity was decreased [24]. Neurotrophic effects of substance P on the hippocampal neurons have been reported [25]. Sleep disturbances such as screaming attacks, fragmented nighttime sleep, and excessive daytime sleeping are also common features in patients with RTT. These symptoms may be due to the decreased levels of melatonin, and in fact, such symptoms are ameliorated by exogenous melatonin treatment [26–28].

2.4. Neurotrophic factors and others

Nerve growth factor (NGF) is known to be a trophic factor, especially for the cholinergic neurons of the basal forebrain. NGF has been shown to be markedly decreased in the CSF of RTT patients, which may explain the decreased brain size [29]. Chen et al. [30] and Martinowich et al. [31] groups found that MECP2 binds selectively to brain-derived neurotrophic factor (BDNF) promoter and functions to regulate expression

of the BDNF gene. Overexpression of BDNF indeed extended the lifespan, restored locomotor activity levels, and relieved some symptoms of the MECP2 mutant phenotype [32,33]. Itoh et al. reported that MECP2 directly regulates expression of insulin-like growth factor binding protein 3 (IGFBP3) gene, which can be expected in turn to inhibit IGF-1 signaling [34,35].

Blue et al. reported significant changes in specific glutamate receptors, including NMDA, AMPA, and metabotropic type glutamate receptors in RTT [36]. Hamberger et al. have reported an elevation in the glutamate level in the CSF of children with RTT [37]. The elevations in NMDA receptors combined with the increased levels of CSF glutamate have suggested that excitatory neurotransmission is enhanced early in the course of the disease. Yamashita et al. measured benzodiazepine binding in stage IV RTT using single-photon computed tomography (SPECT) imaging techniques, and noted a significant reduction in the fronto-temporal cortex, suggesting a decrease in GABA receptors in adult RTT patients [38].

3. Energy metabolism: Rett syndrome is not a mitochondrial disease

Haas et al. have reported elevated CSF lactate and pyruvate in some patients with RTT [39]. Wakai et al. have reported morphological changes in the mitochondria in sural nerve biopsy specimens from patients with RTT [40]. We have also reported that the elevation in CSF lactate levels constituted a secondary biochemical change directly related to the abnormalities in respiration [41,42]. In a related study, we continuously monitored changes in cerebral oxygenation and hemodynamics in the frontal lobes of six patients with Rett syndrome during the awake state, which is associated with hyperventilation (HV) and breath-holding (BH), by near-infrared spectroscopy. We found that oxygenated hemoglobin (HbO₂) and total hemoglobin (HbT) decreased significantly during HV and BH in the awake state compared with the sleep state. The observed continuous decreases in HbO₂ and HbT may cause the focal ischemia and the increased lactate levels in the brain [43]. These findings suggested that RTT was not a primary mitochondrial disorder.

4. Neuropathological study

Armstrong reviewed the neuropathology of RTT and pointed out several important points as follows. The RTT brain is much smaller than a normal brain, and the volume is reduced in specific brain regions including the prefrontal, frontal, and anterior temporal regions. In addition, there are alterations of dendritic arborization in the above brain regions, and some Rett neurons have decreased expression of prealbumin and synaptophysin

immunoreactivity and altered expression of neurotransmitters. Previous neuropathologic studies have also observed decreased melanin content of the zona compacta nigrae in the CNS of RTT patients [44]. Reduced expression of neuropeptides has been observed, including reduced immunoreactivity for tyrosine hydroxylase, a reduction of substance P in the parabrachial complex, and reductions of methionine enkephalin in the brainstem and the basal ganglia [45].

5. Methyl-CpG-binding protein 2 gene

Amir et al. reported on the clinical and laboratory features versus the genotype of MECP2. They also reported that the CSF HVA was significantly decreased in patients with truncating mutations compared with that in patients with missense mutations [46]. Methylation of DNA is essential for development in the mouse and plays an important role in the activation of the X-chromosome, genomic imprinting and gene silencing. The spectrum of MECP2 mutations reflects the importance of the methyl-CpG-binding domain and transcriptional repression domains [47]. Mutation analyses of the MECP2 gene have been performed in Japanese patients with RTT. The T158M mutation is a common mutation in the typical phenotype of RTT [48,49], while the R133C mutation was associated with the mildest cases with preserved speech [46,50]. We have already presented our preliminary clinical and basic research and reviewed the previous literature on RTT [51].

6. Future intervention and therapeutic strategies

6.1. Ghrelin

Ghrelin, a 28 amino acid peptide isolated from the rat stomach as an endogenous ligand for growth hormone secretagogue receptor (GHS-R) 1a and expressed in both the stomach and hypothalamus, exerts multiple physiological functions, including the stimulation of somatic growth, improvement of appetite, and enhancement of the motility of the gut [52]. Many of these functions are related to the clinical phenotypes of RTT, and thus this study investigated the plasma levels of ghrelin in 23 RTT patients in comparison to those in 39 healthy controls. The total ghrelin level in the patients with RTT was 127 ± 71 fmol/ml, and that in the controls was 228 ± 12 fmol/ml; the difference was statistically significant ($P < 0.01$). Thus ghrelin may play an important role in the pathophysiology of RTT.

6.2. MECP2-null mutation mouse model

In collaboration with Kosai et al. we developed an MECP2-null ES cell system using an adenoviral conditional targeting method [53]. We showed the roles of